Classification of Alzheimer's Disease Using Deep Convolutional Spiking Neural Network

Regina Esi Turkson[1,2] ⬤ · Hong Qu[1] · Cobbinah Bernard Mawuli[1] · Moses J. Eghan[2]

Abstract

Diagnosing Alzheimer's Disease (AD) in older people using magnetic resonance imaging (MRI) is quite hard since it requires the extraction of highly discriminative feature representation from similar brain patterns and pixel intensities. However, deep learning techniques possess the capability of extracting relevant representations from data. In this work, we designed a novel spiking deep convolutional neural network-based pipeline to classify AD using MRI scans. We considered three MRI scan groups (patients with AD dementia, Mild Cognitive Impairment (MCI), and healthy controls (NC)). We developed a three-binary classification task (AD vs. NC, AD vs. MCI, and NC vs. MCI) for the AD classification tasks. Specifically, an unsupervised convolutional Spiking Neural Networks (SNN) is pre-trained on the MRI scans. Finally, a supervised deep Convolution Neural Network (CNN) is trained on the output of the SNN for the classification tasks. Experiments are performed using the Alzheimer's Disease Neuroimaging Initiative (ADNI) dataset, and promising results are obtained for the AD classification tasks. We present our proposed model results for both the unsupervised spike pre-training technique and the case where the pre-training technique was not considered, thus serving as a baseline. The accuracy of the proposed model with spike pre-training techniques for the three-binary classification are 90.15%, 87.30%, and 83.90%, respectively, and the accuracy of the model without the spike are 86.90%, 83.25%, and 76.70%, respectively, with a noticeable increase in accuracy and thus, reveals the effectiveness of the proposed method. We also evaluated the robustness of our proposed approach by running experiment on six baseline methods using our preprocessed MRI scans. Our model outperformed almost all the comparable methods due to the robust discriminative capability of the SNN in extracting relevant AD features for the AD classification task.

✉ Regina Esi Turkson
  regina_turkson@yahoo.com; rturkson@ucc.edu.gh

Extended author information available on the last page of the article

1 Introduction

Dementia defines a group of symptoms triggered by ailments of the brain. Alzheimer's Disease (AD), the most prominent of dementia, is an incurable neurological disorder that results in a progressive mental deterioration. This disease can damage brain cells associated with the ability to think and memorize, lose brain function, decrease in mental faculties, problems with language, and a decrease in the ability to construct logical thoughts, and there is no known cure. It starts with a mild decline of nerve cells, which gradually leads to an acute form of dementia, making patients unable to execute their simple day-to-day tasks [1]. With AD, the brain cortex of the patient degenerates, and acute shrinkage occurs particularly in the hippocampus area, the region required in thinking, reasoning, and making new memories [1]. Brain ventricles, which produce cerebrospinal fluid, also become bigger than expected in an AD patient. Individuals diagnosed with mild cognitive impairment (MCI) have a considerably high risk of developing clinical AD, and MCI is often regarded as a transitional phase between healthy cognitive aging and dementia [2, 3]. MCI is a heterogeneous syndrome with unpredictable clinical outcomes. While up to 60% of MCI patients generate dementia within ten years, many people remain cognitively stable or regain normal cognitive (NC) function [4, 5]. According to the Alzheimer's Association, AD is the sixth leading cause of death in the United States [6]. It is caused by many factors, among which age is the most significant. People with age greater than 65 are at a high risk of agonizing from this disease [2].

Although extensive efforts have been made to unveil the pathophysiologic mechanisms of dementia and develop effective treatments, a definitive diagnosis of dementia is typically difficult. Its early diagnosis is crucial for the development of future treatment. Detecting the early stages and the full spectrum of AD progression is essential in order to enable patients to control the risk factors, for example, isolated systolic hypertension before irreversible brain damage develops [7]. To find an effective way of diagnosing AD, some computer-aided systems have been explored to diagnose AD. These systems are designed using machine learning techniques by means of clinical history information and neuropsychological data comprising magnetic resource imaging (MRI), structural MRI (sMRI), functional MRI (fMRI), mini-mental state examination (MMSE), and positron emission tomography (PET) [4]. National Institute of Aging Alzheimer's Association developed the initial clinical criteria for AD diagnosis [8].

Modern researches in computer vision and machine learning are inspired by neural networks and deep learning. Deep Learning is a representation learning method that enables the algorithm to learn distinctive representations from raw data [1]. Deep learning is popular due to its hierarchal and layered structure of the network. Specifically, Deep Convolutional Neural Networks (DCNN) have shown an outperformance for image analysis tasks in recent years. Also, DCNN has inspired neuroscience researchers to start finding solutions to problems associated with neuro-imaging. However, understanding how they work remains an important challenge [9]. Convolutional Neural Networks (CNNs) are inspired by visual imagery [10] and learns the features through a compositional hierarchy of objects, starting with simple edges and moving towards more complex forms through a stack of convolutional and pooling layers [1]. Thus, they can learn high-dimensional non-linear mappings from huge sets of samples, making them perfect for use in image recognition, segmentation, and detection [11]. Some deep learning-based algorithms have recently been implemented to detect AD.

Tong et al. [12] proposed a multi-modal framework that first calculates the pairwise similarity of features for each modality separately and then combines similarities from different modalities into a unified graph for classification using a non-linear graph fusion technique. Likewise, Sorenson et al. [13] joined various MRI biomarkers; cortical thickness measurements, volumetric measurements, hippocampal shape, and hippocampal texture for multi-class classification. Zhang et al. [14] also used a combined kernel technique made by a fusion of features from the three modalities mentioned above with an SVM classifier to classify AD and normal. Liu et al. [4] developed a deep learning framework using a zero-masking strategy for fusing data from different modalities and training a stacked autoencoder (SAE) network for AD classification achieving an accuracy of 87%. In another work, Lui et al. [15] used multi-phase features followed by SAE and a linear softmax classifier by using (Mini-mental State Examination) MMSE as a low-level feature and multi-modal neuroimaging data as a high-level feature. Shi et al. [12] implemented multi-modal Stacked Deep Polynomial Networks (SDPNs) for classification where two separate SDPN learned features from MRI and PET data and the outputs were then merged to a final stage SDPN achieving about 97% accuracy for diagnosing AD from normal.

Payan et al. [16] implemented a deep learning technique made up of sparse autoencoders and pre-trained 3D CNN, which can predict a patient's disease status using MRI scans, achieving an accuracy of 95% while predicting between AD brains and healthy brains. Hosseini et al. [17] expanded the concept of using pre-trained bases and implemented 3D convolutional autoencoders (CAE) with three different scales to capture anatomical shape variations in structural brain MRI scans to predict AD. Multiple fully connected layers were used on top of convolutional layers for class evaluations improving the accuracy to 94%. However, Sarraf et al. [18] were the first to implement the diagnosing pipeline with pure CNN without any pre-training. They trained their network to differentiate Alzheimer's MRI and fMRI from normal healthy control data for a given age group using LeNet and GoogLeNet models and achieved the best results for binary classification. Danni et al. [19] constructed multiple deep 3D convolutional neural networks (3D-CNNs) to learn the various features from local brain images for the classification of AD diagnosis.

Spiking Neural Networks (SNNs) are brain-inspired ANN models that are fast becoming a promising candidate for neuromorphic computing due to better energy efficiency as a result of sparse event-driven and asynchronous information processing and their notable inference accuracy in numerous cognitive tasks such as image classification and speech recognition [20, 21]. Training SNNs remains a difficult task as compared to training ANNs. The main reason being the discontinuous activation function, which avoids direct usage of gradient-based optimization. Regardless of the non-differentiable nature of SNN activations, several workarounds allow the use of backpropagation algorithms in most scientific literature [22]. Currently, efforts are being made in SNNs, focusing on implementing deeper networks with multiple hidden layers to incorporate exponentially more challenging functional representations [20]

While promising results have been recounted for SNN and brain image analysis, there is still room for further research to uncover some limitations in this domain's feature extraction methods.

The literature above gives a substantial overview of current trends in the classification of different brain imaging modalities in the problem of computer-aided diagnostics of AD and its prodromal stage, i.e., mild cognition impairment (MCI). With motivation from these literature, we design a novel diagnostic architecture for AD classification using Spiking Deep Convolutional Neural Networks (CNNs). We implemented an architecture of a spiking deep CNN-based multi-class pipeline for classifying complex dynamic brain

activities. A three-binary classification task (AD vs. NC, AD vs. MCI, and NC vs. MCI) model for AD classification is proposed. Specifically, an unsupervised convolutional Spiking Neural Networks (SNN) is pre-trained on the MRI scans, and a supervised deep Convolution Neural Network (CNN) is trained on the output of the SNN for the classification tasks. Our proposed model was implemented using BindsNET [23], a Python package built on the PyTorch deep neural networks library to simulate SNNs. Comparatively, we experimented the robustness of our proposed approach on some classical machine learning methods using our preprocessed MRI scans. Our model outperformed almost all the comparable methods due to the robust discriminative capability of the SNN in extracting relevant AD features for the AD classification task. Inspired by these literatures, specifically, classifying AD with a prior unsupervised deep learning model and the novel performance of spiking neural networks in image classification tasks, the main contributions of this work are:

To the best of our knowledge, this work is the first deep learning framework to classify AD with spiking neural network.

It provides an automatic end-to-end approach to classify AD.

The rest of the paper is organized as follows; Section II presents the methodology and implementation of the proposed model, highlighting the architecture of the spiking deep CNN. In Section III, we show the experimental setup and results of our proposed model with an unsupervised spike pre-training technique, and the case where the pre-training technique was not considered. Section IV and Section V contains the discussion and conclusion of our work, respectively.

2 Methodology and Implementation

In our proposed model, we developed a two-stage AD classification framework using preprocessed MRI scans. Specifically, the proposed methodology consists of two parts: (1) An unsupervised convolutional SNN model to extract discriminative AD features; and (2) A supervised deep convolutional neural network that finally predicts the AD group using the output from the SNN. Figure 1 shows the general framework for our proposed model.

2.1 Subjects

The dataset used in this research was attained from the Alzheimer's Disease Neuroimaging Initiative (ADNI) database (http://adni.loni.usc.edu/methods/documents). The ADNI is a public project that makes reliable clinical and imaging data available to researchers of AD. In this study, we included a total of 450 participants from the ADNI database. The
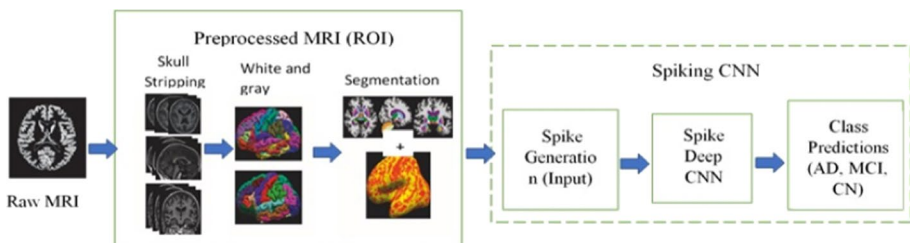
Fig. 1 General Overview Architecture of Proposed Model

dataset includes subjects from ADNI-1, ADNI-2, and ADNI-GO, who had baseline T1 and T2 weighted scans. We included three groups of participants, each group with 150 subjects: cognitively normal persons (Mini-Mental State Examination (MMSE) > 24, Clinical Dementia Rating (CDR) = 0, non-depressed), patients with Alzheimer's disease (MMSE < 26, CDR > 0.5), and patients with mild cognitive impairment (MMSE > 24, CDR = 0.5, with objective memory loss). The demographic information of the dataset is presented in Table 1.

2.2 MRI Acquisition Protocol and Data Preprocessing

Structural T1-weighted and T2-weighted MRI scans were attained using 1.5 T and 3 T scanners. The following sequences were acquired: (1) 1.5 T T1-weighted; acquisition parameters were repetition time (TR) = 2400 ms, minimum full echo time (TE), inversion time (TI) = 1000 ms, flip angle = 8° or 9°, field-of-view (FOV) = 240 × 240 mm2, slice thickness = 2 mm, acquisition matrix with varying x, y, and z dimensions; (2) 1.5 T T2-weighted; 3 T scans, the acquisition parameters were a TR = 2300 ms, minimum full TE, TI = 900 ms, flip angle = 8° or 9°, FOV = 260 × 260 mm2, slice thickness = 3 mm or 4 mm, and varying acquisition matrix. Slices of all anatomical planes were obtained. (3) 3 T T2-weighted; repetition time (TR) = 3000 ms, echo time (TE) = 85 ms, flip angle = 90°, slice thickness = 3 mm, the field of view [FOV] = 230 × 208 mm2, matrix size = 256 × 242).

Aforementioned, the dataset used in this study was obtained from Alzheimer's disease Neuroimaging Initiative (ADNI) [24]. MRI scans are provided in the form of 3D Nifti volumes. The original structural magnetic resonance imaging (sMRI) images, both T1 and T2 weighted, were obtained from 1.5 T or 3 T scanner machines (using General Electric (GE) Medical System, Philips Medical Systems, and Siemens MRI scanners) in all centers. We preprocessed the raw MRI scans to transform the original multicenter brain images into standard image space so that the same brain substructures can be registered at the same image coordinates for different participants.

The MRI scans were preprocessed using the typical procedures of Anterior Commissure (AC), Posterior Commissure (PC) correction, skull-stripping, and brain parcellation in 138 anatomical structures. Before extracting the region of interest (ROI), the geometric normalization task has to be executed on the image dataset to align the images with the Montreal Neurological Institute (MNI) template, representing an average of 152 individual brain scans. To select the ROI, a brain atlas termed AAL that corresponds to the used MNI template was used. We used ACPCDETECT [25] program, an Automatic Registration Toolbox (ART), to automatically align the images. The alignment was gathered using affine (rigid

Table 1 Demographic and clinical characteristics		AD	MCI	NC
	Sex (M/F)	65/85	96/54	77/73
	Age (y)	75.2 ± 7.2	71.4 ± 6.2	65.2 ± 4.0
	CDR	1.2 ± 0.5	0.5 ± 0.2	0 ± 0
	MMSE	18.09 ± 5.55	27.40 ± 1.70	29.10 ± 1.0

Values are shown as mean ± SD

AD, Alzheimer's disease patient; MCI, Mild cognitive impairment; NC, Cognitively normal patient; MMSE, Mini-Mental State Examination; CDR, Clinical Dementia Rating

body) registration. The program takes a 3D structural MRI of the human brain as input. It automatically detects the mid-sagittal plane (MSP), then detects the Anterior Commissure and Posterior Commissure intersection points, and finally, it detects eight additional landmarks (the Orion landmarks) on the MSP. This information is used to tilt-correct the input volume into a standard orientation. After the alignment, every subset of images was manually verified to guarantee the correct procedure using the FSLeyes software [26]. The aligned MRI scans are then reformed to $60 \times 60 \times 60$ using the Statistical Parametric Mapping (SPM) toolbox (Penny et al., 2011). Furthermore, spatial normalization was applied to the images to match them in the MNI152 template. Diluted or enhanced intensity was implemented to compensate for the structural alterations.

A brain parcellation was then executed to acquire all brain structures needed for this work. This was performed over all available images utilizing multi-atlas label propagation with expectation–maximization based refinement (MALPEM) [27]. This tool is a state-of-the-art automatic segmentation technique for the robust segmentation of whole-brain MR images into 138 unique anatomical structures. The MALPEM has five principal modules to do the brain parcellation; N4 bias correction, pincram brain extraction, label propagation, label fusion, and label refinement. We found out that the Entorhinal Area, Amygdala, Hippocampus, and the Posterior Cingulate Cortex were the discriminator's best set. We used these four (4) ROIs for the classification. Processed slices for each class are presented in Fig. 1.

Once the preprocessing stage is done, all the data extracted were normalized to zero mean and unit variance for each feature by a standard scalar function. That is, given the data matrix A, where rows denote subjects and columns denote features, the normalized matrix with elements $a(i,j)$ is given by.

$$A norm(i,j) = \frac{a(i,j) - mean(a_j)}{std(a_j)} \tag{1}$$

where A_j is the jth column of the matrix (A).

2.3 Network Architecture

We show our proposed network architecture, which comprises a pre-trained spiking neural network and a deep convolutional neural network in this section.

2.3.1 Unsupervised Pre-training with Convolutional Spiking Neural Network

Spiking Neural Networks (SNNs) are a major research domain in theoretical neuroscience and neuromorphic engineering that uses event-based, data-driven updates to maximize efficiency, especially if inputs from event-based sensors are joined [25]. This minimized redundant information based on asynchronous event processing. In theory [26], SNNs are as computationally powerful as conventional Artificial Neural Networks. SNN cannot directly calculate analog; hence we first need to encode the analog value to the spike's timing, input it into SNN, and then output the expected results in the spike mode [27]. In this work, the time-to-first-spike coding strategy is implemented on the SNN for the unsupervised pre-training and a non-linear function that perceives the corresponding relationship from the preprocessed MRI pixel values

to the spike times of the neurons. The conversion between the original image pixels and the firing time of neuronal spikes using the sigmoid function is represented as:

$$t = \frac{T_{max}}{1 + \exp(\sigma(128 - p))} \tag{2}$$

where p are the image pixels in the interval, t denotes spike's firing time, σ is the non-linear coding parameter, T_{max} is the maximum firing time, with a set value of 50 ms.

The SNN in this architecture comprises four layers. The first layer is the input layer, made up of 464×464 neurons (one neuron per image pixel); the second, third, and four layers are the processing layers, having a variable number of excitatory neurons and many inhibitory neurons. Each input is a Poisson spike, which is input to the successive layers' excitatory neurons (i.e., second, third, and fourth layers). The MRI scans are presented to the network for 50 ms in the form of Poisson-distributed spike trains, with firing rates proportional to the intensity of the scans' pixels. Specifically, the maximum pixel intensity for input firing rates is set between 0 and 128 Hz. The excitatory neurons of these layers are linked in a one-to-one fashion to inhibitory neurons; thus, each spike in an excitatory neuron triggers a spike in its matching inhibitory neuron. The second, third, and fourth layers are in the form of quasi-convolutional spike layers. The spike stride, number of filters, and kernel size are 32, 25, and 128, respectively. Each of the inhibitory neurons is linked to all excitatory ones, except for the one from which it receives a connection. The connectivity offers lateral inhibition and establishes competition among excitatory neurons. The SNN architecture has simple spike-timing-dependent plasticity (STDP) rule between the input and excitatory neurons and a competitive inhibition technique to learn prototypical AD filters from the MRI scans using the [28] technique between the second and the fourth layer. It is worth noting that all synapses from input neurons to excitatory neurons are learned using the power-law weight dependence STDP rule. With the STDP rule, the spike signals $s_i(t)$ are modeled as either 0 or 1 in one millisecond (ms) time increments. Specifically, 1 ms pulse of unit amplitude represents a spike while 0 represents no spike. In each kth input neuron, we control the STDP rule with a memory potential, $V(t)$ represented as.

$$V(t) = \sum_{k=1}^{N} w_k s_k(t) \tag{3}$$

where w_k is the associated weight (synapse) of the input neuron, and $w_k s_k(t)$ forms a postsynaptic potential. if the membrane potential $V(t)$ at time t is greater than a specified threshold, ρ, i.e., if.

$$V(t) > \rho \tag{4}$$

then the output neuron spikes.

To increase simulation execution speed, the weight dynamics are calculated using synaptic traces. Meaning, despite the synaptic weight, each synapse keeps track of a value, namely the presynaptic trace, which simulates the recent presynaptic spike history. Whenever a presynaptic spike reaches the synapse, the trace is increased by 1; otherwise, it decays. Weight updates are generated only when a postsynaptic excitatory neuron fires a spike. The unsupervised SNN is trained with a random backpropagation approach. The cost function L_{sp} defined as

$$L_{sp} = 0.5 \sum_{i} (v_i^p(t) - v_i^l(t))^2 \tag{5}$$

in the network has the weights (W_{ij}) update representation as

$$\frac{\partial L_{sp}}{\partial W_{ij}} = -\sum_i e_i(t) \frac{\partial v_i^p(t)}{\partial W_{ij}} \quad (6)$$

where $e_i(t)$ is the ith output neuron error, v^p and v^l are the firing rates of the prediction neuron and the labeled neuron. Equation 6 is further decomposed as

$$\Delta W_{ij}^c \propto \begin{cases} -\sum_k g_{ik} e_k^E \, if s_j^C(t) \text{ and } & b_{min} < I_i(t) < b_{max} \\ 0 & otherwise \end{cases} \quad (7)$$

where $I_i(t)$ is the current entering the ith neuron, b_{min} and b_{max} are the minimum and maximum boundary for $I_i(t)$, $s_j^C(t)$ indicates the presence of a presynaptic spike, e_k^E represents the error term of kth the neuron in the output layer, and g_{ik} is a fixed random number in the random backpropagation algorithm. The unsupervised spike neural network is trained for 20 iterations. For the spiking implementation, (hyper)parameters obtained from a coarse manual search are identical to previous work [29].

The fourth layer's output, which has a $50 \times 464 \times 464$ dimension, is fed into the supervised convolutional deep learning model. The output features are considered the relevant extracted AD features from the network. We used BindsNET [20] library to construct the unsupervised SNN model. The overall unsupervised pre-training network is shown in Fig. 2.

2.3.2 AD Classification with Deep Convolutional Neural Network

We model a Deep Convolutional Neural Network (DCNN) architecture for the classifying AD. In Convolutional Neural Networks (CNNs), image features are presented as inputs to its hierarchical structure's lowest layer. The complex nature of CNN architecture provides a level of invariance convolutional operations. The local receptive field ensures the neurons' access to elementary features, such as oriented edges or corners [19]. The convolutional layer is the essential building block in a network, primarily comprising neurons having learnable weights and biases. The convolutional layer's parameters contain a set of learnable filters. Each filter is spatially small but varies through the full depth of the input volume. Each filter is convolved across the input volume's
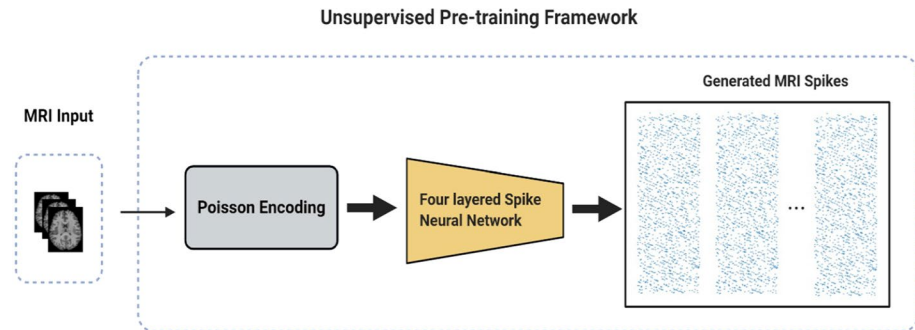

Fig. 2 Unsupervised AD Pre-training with spike neural network

width and height, generating an activation map of that filter. During this convolving, the network learns the activated filters when a specific type of feature at some spatial position in the input is realized. Next, these activation maps for every filter is stacked along the depth dimension, producing the full output volume. It also contains other network structures, such as a pooling layer, which implements downsampling operation along the spatial dimensions. Refer to [19, 28] for a description of CNN. For training the CNN architecture, a categorical cross-entropy loss (L_c) function is used. The cross-entropy function measures a classification model's performance whose output is a probability value between 0 and 1. Cross-entropy loss rises as the expected output diverges from the actual label. For a binary classification task, the cross-entropy loss is calculated as:

$$L_c^m = -(p_m \log y_m + (1 - p_m) \log(1 - y_m)) \tag{8}$$

where m is the data (MRI) sample instance, p_m and y_m the predicted and actual class value for the data sample.

The convolutional deep learning model consists of five 3×3 Conv layers with 8, 16, 32, 32, and 64 feature maps, respectively. The last convolutional layer is followed by a flatten layer with shape 1×3136 and two fully connected layers with 64 and 2 nodes. Except for the third convolutional layer, each of the convolutional layers is followed by a Rectified Linear Unit (ReLU) activation layer and 2×2 max-pooling, and an adaptive average pooling layer only for the last convolutional layer of size (7×7). A max-pooling layer followed the convolutional operations to reduce successive outputs' dimensions to ensure computer memory's effective utilization. We applied a dropout of 0.50 after the second fully connected layer. Finally, we applied a soft-max after the last fully connected layer to output the predicted AD group's probability. The proposed network has a total of 0.23 million parameters. The SNN learning model is trained before the supervised learning model to extract discriminative features of MRI scans. In this DCNN model, the Adam optimizer was used for the model training with a mini-batch size of 5, $\beta_1 = 0.9$, and $\beta_2 = 0.99$ an initial learning rate of 1×10^{-4}. Almost all the AD classification tasks' training reached a convergence state within 200 training epochs in the experiment. We evaluated the trained model on the test set and considered this as the performance with various performance metrics. The detailed architecture configuration is shown in Fig. 3 and Table 2.
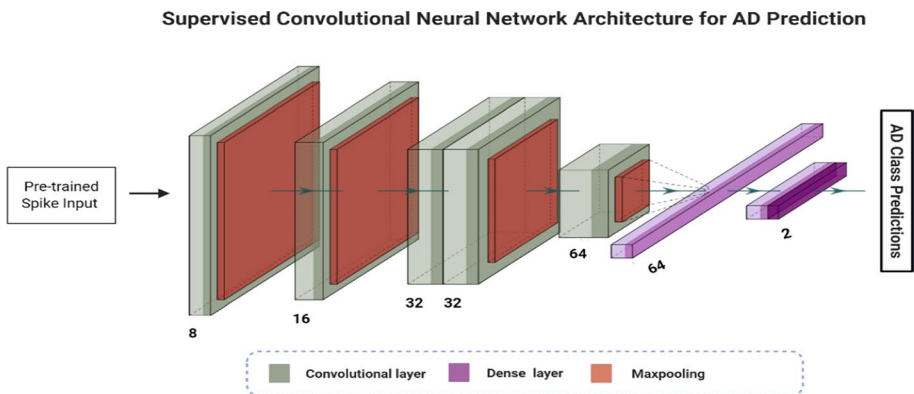

Fig. 3 Supervised convolutional neural network architecture for AD prediction

Table 2 Architecture configuration for the supervised network architecture

Layer name	Kernel size/ Pool Size	Stride Size	Filter	Output Shape	Parameters
conv2d	3 ×3	1 × 1	8	$8 \times 464 \times 464$	80
max2d	2 × 2	2 × 2	–	–	0
conv2d	3 ×3	1 ×1	16	$16 \times 232 \times 232$	1168
max3d	2 ×2	2 × 2	–	-	0
conv3d	3 ×3	1 ×1	32	$32 \times 116 \times 116$	4640
conv3d	3 × 3	1 × 1	32	$32 \times 116 \times 116$	9240
max3d	2 ×2	2 × 2	–	–	0
conv3d	3 × 3	1 × 1	64	$64 \times 58 \times 58$	18,496
max3d	2 ×2	2 × 2	–	–	0
adaptiveAverage2dPool	–	–	–	$64 \times 7 \times 7$	0
flatten	–	–	–	1×3136	0
Dense(fully)	–	–	64	1×64	200,768
Dense(fully) + softmax	–	–	2	1×2	130

3 Comparison Methods

We evaluate the robustness of our proposed approach for AD classification with six baseline methods. Precisely, we thoroughly run experiments with these methods on the preprocessed MRI scans for all baseline methods. The baseline methods are sparse autoencoders and 3D convolutional neural networks [30, 31], 3D CNN [29], Support Vector Machine (SVM) [32], Random Forest (RF) [33], KNN [34] and Naïve Bayes (NB) [35]. Empirical results by these methods are reported in the experiments and results sections.

4 Experiments and Results

4.1 Experimental Setup

The evaluation of our proposed methods is conducted on three-binary classification tasks: (1) AD vs. NC, (2) MCI vs. NC, and (3) AD vs. MCI. The MRI scans were normalized into a range of 0 to 1 using Eq. 1. The performance of our approach is evaluated with the following metrics: accuracy $(ACC) = (TP + TN)/ (TP + TN + FN + FP)$, specificity $(SPE) = TN/ (TN + FN)$, and sensitivity $(SEN) = TP/ (TP + FN)$. FP, TP, FN, and TN represent false-positive, true-positive, false-negative, and true-negative classification results. Thus, if an AD patient is classified as AD, this is deemed a TP and otherwise as FN. Also, TN denotes the number of normal subjects classified into the normal group, and FP denotes otherwise. We used a total of 450 MRI scans with a training dataset ($N = 130$) and a test dataset ($N = 20$) for each of the MRI data classes (AD, MCI, NC). We used BindNET to build the SNN for pre-training the spikes and Pytorch for the deep CNN for the binary classification.

4.2 Results

In Table 3, we present our proposed model's results with an unsupervised spike pre-training technique and the case where the pre-training technique was not considered (See Fig. 4 and Fig. 5). The results clearly show the importance of unsupervised spike learning, which helps the model learn significant discriminative representations in high-dimensional space before applying the supervised learning. The three-binary classification tasks reported are AD vs. NC, AD vs. MCI, and NC vs. MCI. The highest accuracy, sensitivity, and specificity (90.15, 96.50, and 87.12, respectively) were obtained in the AD vs. NC classification tests for the proposed approach using the unsupervised SNN.

5 Discussion

We discuss the results with other model, in terms of accuracy, sensitivity, and specificity. It is worth noting that while the other comparative models may have used different dataset size, and different experimental setups, the results are still comparable since all the models reported their outcomes with structural MRI scans, which have close similarity across datasets, especially when the MRI scans have been preprocessed and the brain have been registered and segmented in the published works.

The significant effect of the unsupervised SNN can be seen in our reported results. In Table 3, it could be seen that our proposed model outperformed almost all the performance metrics (except for specificity) of the comparative published state-of-the-art works. The works by MKSM [10], SAE [10], MPFR [10], and SAE [9] though were designed with convolutional neural networks, lack the full capability to extract relevant discrimination AD representative features to classify the AD groups with very promising confidence. Furthermore, SAE [9] and 3D CNN [30] also applied the idea of unsupervised pre-training, but with sparse autoencoder before finally performing the AD classification task. The sparse autoencoder, though, extracted some relevant AD features for AD classification but was not efficient enough to register an excellent performance on all the AD classification tasks, comparable to our proposed pre-training with a convolutional spike neural network. For the classical machine learning methods (NB, RF, KNN and SVM), it could be noticed that it registered the worse performance because of its inability to learn significant data patterns with high dimensional space specifically for the MRI data.

Our proposed method outperformed almost all the comparable methods due to the robust discriminative capability of the SNN in extracting relevant AD features for the AD classification task. Our models' promising results are due to the SNN and the capabilities of the supervised convolutional neural network picking the most informative AD patterns from the output of the unsupervised model. Combining these two techniques produced an outstanding performance with a comparatively smaller training dataset for AD classification.

Table 3 Comparable classification performance(%) for the proposed method and other state-of-the art methods for ad classification

Method	AD vs. NC			AD vs. MCI			NC vs. MCI		
	ACC	SEN	SPE	ACC	SEN	SPE	ACC	SEN	SPE
MKSM [15]	89.60±0.91	89.09±1.39	90.10±1.12	–	–	–	–	–	–
SAE [15]	88.20±7.68	87.66±9.50	87.50±15.04	–	–	–	–	–	–
MPFR [15]	90.11±3.06	84.45±10.51	93.89±6.31	–	–	–	–	–	–
SVM [7]	–	–	–	–	–	–	71.27±3.26	47.02±12.37	84.50±4.25
SAE [7]	–	–	–	–	–	–	71.98±5.48	49.52±13.68	84.31±13.15
SVM[31]	70.48±1.30	100±0	51.12±3.0	66.66±0.45	100±0	48.0±5.30	62.05±1.15	100±0	47.0±4.20
KNN[34]	69.37±0.34	94.76±1.15	47.18±6.81	66.16±1.80	93.75±0.20	47.25±5.0	77.77±2.10	84.66±2.0	67.36±2.15
RF[32]	75.64±1.23	91.62±0.50	30.75±10.12	67.08±1.65	100.0±0	47.20±4.23	46.15±7.30	46.10±11.10	100±0
NB[33]	52.76±5.0	50.26±6.12	58.5±4.25	63.75±0.34	93.75±0.12	41.00±6.17	47.08±8.12	51.21±7.16	85.16±1.15
3D CNN[30]	91.12±1.5	94.12±1.5	84.23±0.4	87.10±1.30	88.70±1.20	83.21±1.2	82.07±1.78	82.04±0.67	81.23±0.12
3DAE+CNN [29]	86.15±1.26	90.0±0.88	73.0±2.34	86.00±0.95	100±0	69.12±1.67	81.12±0.46	99.13±0.23	66.72±1.76
Without Spike	86.90±2.1	89.72±2.3	82.20±1.4	83.25±1.2	85.56±2.1	86.48±1.5	76.70±2.0	84.90±1.6	72.89±1.3
Ours	**90.15±1.1**	**96.50±2.4**	**87.12±1.2**	**87.30±1.4**	**90.20±1.1**	**85.30 + 1.3**	**83.90±2.5**	**88.90±1.3**	**75.63±2.4**

ACC, Accuracy; *SEN*, Sensitivity; *SPE*, Specificity
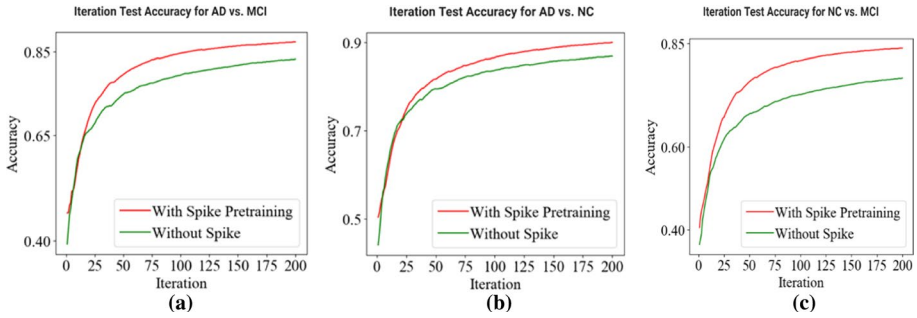
Fig. 4 Iteration test accuracy for **a** AD vs. MCI **b** AD vs. NC and **c** NC vs. MCI
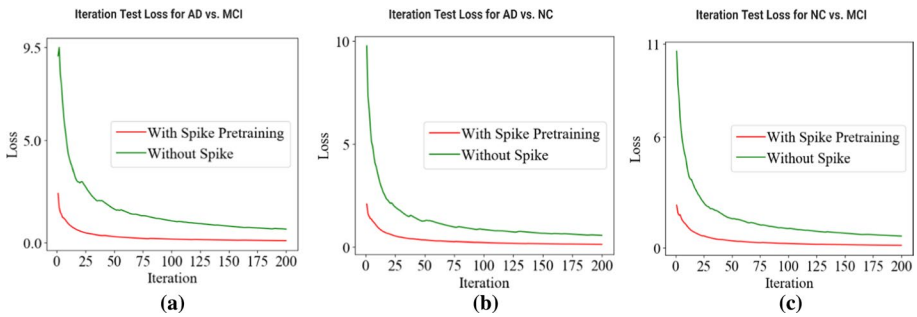

Fig. 5 Iteration test loss for **a** AD vs. MCI **b** AD vs. NC and **c** NC vs. MCI

6 Conclusion

This study proposed a spiking deep convolutional network-based framework for classifying MRI images to detect Alzheimer's disease. Specifically, three binary classification tasks (AD vs. NC, AD vs. MCI, and NC vs. MCI) were performed. Experimental data was obtained from ADNI, and a total of 450 MRI scans were used. Firstly, the MRI scans were preprocessed, including skull-striping, registration, segmentation, and region of interest outlining. The preprocessed images were pre-trained with an unsupervised spiking neural network to extract significant AD features. The pre-trained spikes were then passed to the deep CNN network for the classification task. The SNN was trained and tested using our model (pre-trained with spike) and model without a pre-trained spike. Experimental results from our model outperformed the other baseline models. Pre-trained feature learning using spikes in the network facilitated accurate prediction of the three binary classification tasks. SNN improved the performance gain, demonstrating the potential of incorporating spiking deep models directly from scratch for learning distinct features from neuroimaging data and has a high-level of effects for medical and neuroimage processing. Such systems are reliable and consistent as well as error-free. Future work may include merging patients' clinical data with imaging data and dealing with multi-modal data to construct a more robust SNN system for predicting AD cases.

Data and Code Availability The ADNI data used for this research will be made available upon request to the corresponding author and the Alzheimer's Disease Neuroimaging Initiative (ADNI) committee. The algorithms were written in Python using Pytorch and BindsNet. The algorithm implementation for this paper is publicly available at (https://github.com/mvisionai/AdSpike).

Declarations

Conflict of interest The authors report no competing interests.

References

1. Farooq A, Anwar S, Awais M, Rehman S (2017) A deep CNN based multi-class classification of Alzheimer's disease using MRI. In: International Conference on Imaging systems and techniques IST 2017 vol. 2018-Janua, pp. 1–6
2. Korolev IO (2014) Alzheimer 's disease : a clinical and basic science review. Med Stud Res J 04(September):24–33
3. Verwoerd JH, Mattace-Raso FUS (2012) Mild cognitive impairment. Huisarts Wet 55(10):464–467
4. Luo S, Li X, Li J (2017) Automatic Alzheimer's disease recognition from mri data using deep learning method. J Appl Math Phys 05(09):1892–1898
5. Mitchell AJ, Shiri-Feshki M (2009) Rate of progression of mild cognitive impairment to dementia - Meta-analysis of 41 robust inception cohort studies. Acta Psychiatr Scand 119(4):252–265
6. Gaugler J, James B, Johnson T, Scholz K, Weuve J (2016) 2016 Alzheimer's disease facts and figures. Alzheimer's Dement 12(4):459–509
7. Liu S et al (2015) Multimodal neuroimaging feature learning for multiclass diagnosis of Alzheimer's disease. IEEE Trans Biomed Eng 62(4):1132–1140
8. McKhann GM et al (2011) The diagnosis of dementia due to Alzheimer's disease: recommendations from the National Institute on Aging-Alzheimer's Association workgroups on diagnostic guidelines for Alzheimer's disease. Alzheimer's Dement 7(3):263–269
9. Islam J, Zhang Y (2019) Understanding 3D CNN behavior for Alzheimer's disease diagnosis from brain PET scan. pp 3–6. arXiv: 1912.04563
10. Yann L, Yoshua B (1995) Convolutional networks for images, speech, and time-series. Handb Brain Theory Neural Netw 4:2571–2575
11. Roy SS, Sikaria R, Susan A (2020) A deep learning based CNN approach on MRI for Alzheimer's disease detection. Intell Decis Technol 13(4):495–505
12. Shi J, Zheng X, Li Y, Zhang Q, Ying S (2018) Multimodal neuroimaging feature learning with multimodal stacked deep polynomial networks for diagnosis of Alzheimer's disease. IEEE J Biomed Heal Inform 22(1):173–183
13. Sørensen L et al (2017) Differential diagnosis of mild cognitive impairment and Alzheimer's disease using structural MRI cortical thickness, hippocampal shape, hippocampal texture, and volumetry. NeuroImage Clin 13:470–482
14. Zhang D, Wang Y, Zhou L, Yuan H, Shen D (2011) Multimodal classification of Alzheimer's disease and mild cognitive impairment. Neuroimage 55(3):856–867
15. Liu S, Liu S, Cai W, Pujol S, Kikinis R, Feng DD (2015) Multi-phase feature representation learning for neurodegenerative disease diagnosis. Lect Notes Comput Sci including Subser Lect Notes Artif Intell Lect Notes Bioinform 8955:350–359
16. Payan A, Montana G (2015) Predicting Alzheimer's disease a neuroimaging study with 3D convolutional neural networks. In: ICPRAM 2015 - 4th international conference pattern recognition applied methods, Proc., vol. 2, pp. 355–362
17. Hosseini-Asl E, Keynton R, El-Baz A (2016) Alzheimer's disease diagnostics by adaptation of 3D convolutional network. In: 2016 IEEE International Conference on Image Processing. IEEE, pp 126–130
18. Sarraf S, DeSouza D, Anderson J, Toighi J (2016) DeepAD: Alzheimer's disease classification via deep convolutional neural networks using MRI and fMRI. bioRxiv 070441. https://doi.org/10.1101/070441
19. Cheng D, Liu M, Fu J, Wang Y (2017) Classification of MR brain images by combination of multi-CNNs for AD diagnosis. In: Ninth International Conference on Digital Image Processing (ICDIP 2017), vol. 10420, no. Icdip, p. 1042042, 2017.

20. Lee C, Panda P, Srinivasan G, Roy K (2018) Training deep spiking convolutional Neural Networks with STDP-based unsupervised pre-training followed by supervised fine-tuning. Front Neurosci 12:435. https://doi.org/10.3389/fnins.2018.00435

21. Turkson RE, Qu H, Wang Y, Eghan MJ (2020) Unsupervised multi-layer spiking convolutional neural network using layer-wise sparse coding, vol 12534. Springer International Publishing, LNCS

22. Ledinauskas E, Ruseckas J, Juršenas A, Buračas G (2020) Training deep spiking neural networks. arXiv: 2006.04436

23. Hazan H et al (2018) BindsNET: a machine learning-oriented spiking neural networks library in python. Front Neuroinform 12(December):1–18

24. Jack CR et al (2008) The Alzheimer's disease neuroimaging initiative (ADNI): MRI methods. J Magn Reson Imaging 27(4):685–691

25. Ardekani BA, Bachman AH (2009) Model-based automatic detection of the anterior and posterior commissures on MRI scans. Neuroimage 46(3):677–682

26. Jenkinson M, Bannister P, Brady M, Smith S (2002) Improved optimization for the robust and accurate linear registration and motion correction of brain images. Neuroimage 17(2):825–841

27. Ledig C, Wolz R, Aljabar P, Jyrki L (2012) Multi-class brain segmentation using atlas propagation and EM-based refinement Department of Computing , Imperial College London , London , UK Knowledge Intensive Services , VTT Technical Research Centre of Finland , Tampere , Finland The Neurodis Foundat, pp. 896–899

28. Diehl PU, Neil D, Binas J, Cook M, Liu SC, Pfeiffer M (2015) Fast-classifying, high-accuracy spiking deep networks through weight and threshold balancing. In: Proceedings of the international joint conference on neural network, vol. 2015 Sept 2015.

29. Xing X, et al. (2020) Dynamic image for 3d mri image alzheimer's disease classification. In: European conference on computer vision. Springer, Cham

30. Hosseini-Asl E, Keynton R, El-Baz A (2016) Alzheimer's disease diagnostics by adaptation of 3D convolutional network. In: 2016 IEEE international conference on image processing (ICIP). IEEE

31. Islam, Jyoti, and Yanqing Zhang (2019) Understanding 3D CNN behavior for Alzheimer's disease diagnosis from brain PET scan. arXiv preprint arXiv:1912.04563

32. Zhao Q et al (2018) Evaluating functional connectivity of executive control network and frontoparietal network in Alzheimer's disease. Brain Res 1678:262–272

33. Maggipinto T et al (2017) DTI measurements for Alzheimer's classification. Phys Med Biol 62(6):2361

34. Wasule V, Poonam S (2017) Classification of brain MRI using SVM and KNN classifier. In: 2017 third international conference on sensing, signal processing and security (ICSSS). IEEE

35. Gupta Y, et al. (2019) Alzheimer's disease diagnosis based on cortical and subcortical features. J Healthc Eng

Authors and Affiliations

Regina Esi Turkson[1,2] 🔟 **· Hong Qu[1] · Cobbinah Bernard Mawuli[1] · Moses J. Eghan[2]**

Hong Qu
hongqu@uestc.edu.cn

Cobbinah Bernard Mawuli
cobbinahben@std.uestc.edu.cn

Moses J. Eghan
meghan@ucc.edu.gh

1   School of Computer Science and Engineering, University of Electronic Science and Technology of China, Chengdu 611731, China

2   Department of Computer Science and Information Technology, University of Cape Coast, PMB University Post Office, Cape Coast, Ghana